BULLETIN OF THE POLISH ACADEMY OF SCIENCES
TECHNICAL SCIENCES, Vol. 62, No. 4, 2014
DOI: 10.2478/bpasts-2014-0073

Dedicated to Professor Jan Dorosz
on the occasion of his 65th birthday

Stack and draw fabrication of soft glass microstructured fiber optics

D. PYSZ[1], I. KUJAWA[1], R. STĘPIEŃ[1], M. KLIMCZAK[1], A. FILIPKOWSKI [1], M. FRANCZYK[1], L. KOCISZEWSKI [1], J. BUŹNIAK[1], K. HARAŚNY[1], and R. BUCZYŃSKI[1,2*]

[1] Institute of Electronic Materials Technology, 133 Wólczyńska St., 01-919 Warsaw, Poland
[2] Faculty of Physics, Warsaw University, 7 Pasteura St., 02-093 Warsaw, Poland

Abstract. A broad review is given of microstructured fiber optics components – light guides, image guides, multicapillary arrays, and photonic crystal fibers – fabricated using the stack-and-draw method from various in-house synthesized oxide soft glasses at the Glass Department of the Institute of Electronic Materials Technology (ITME). The discussion covers fundamental aspects of stack-and-draw technology used at ITME, through design methods, soft glass material issues and parameters, to demonstration of representative examples of fabricated structures and an experimental characterization of their optical properties and results obtained in typical applications. Specifically, demonstrators include microstructured image guides providing resolution of up to 16000 pixels sized up to 20 μm in diameter, and various photonic crystal fibers (PCFs): index-guiding regular lattice air-hole PCFs, hollow core photonic bandgap PCFs, or specialty PCFs like highly birefringent microstructured fibers or highly nonlinear fibers for supercontinuum generation. The presented content is put into context of previous work in the area reported by the group of authors, as well as other research teams.

Key words: soft glass, stack and draw, image guide, photonic crystal fiber, microstructured fiber, nonlinear optics.

1. Introduction

The Glass Department at the Institute of Electronic Materials Technology (ITME) has been involved in research and development of structured fiber optics elements for optoelectronics for the past two decades. Specifically, the classes of components, which can be developed at ITME with presently disposed fabrication capabilities and expertise include: fiber optic lightguides, image guides, fiber optic plates (FOP), lenses, tapers, twisters, multicapillary arrays, photonic crystal fibers (PCF), photonic bandgap fibers (PBG), microstructured fibers with special properties (active photonic fibers, sensing fibers, highly nonlinear fibers). All these elements, due to their particular properties, play significant roles in optoelectronics. Some of them are widely used in the optical devices: fiber optic plates, twisters, tapers – night vision, electronic image intensifiers (EII), low light level cameras and similar; fiber optic lightguides – biostimulation lasers, dental curing lamps; image guides – medical and technical borescopes; multicapillary arrays – filtration, nebulization, particle and X-ray optics. PCF and PBG fibers are now intensively investigated. They demonstrate very interesting properties enabling to overcome the limitations of conventional fibers. For example: endlessly single mode guiding, large core single mode fibers, guidance in hollow air core (due to photonic band gap effect, PBG), very high birefringance, nonlinear properties, flat dispersion and near-zero dispersion, high $\chi^{(3)}$ nonlinearity for ultra-broadband radiation sources (supercontinuum). The main advantage of photonic fibers is the possibility of shaping the propagation properties by manipulating parameters of the fiber's transverse structure – diameter of holes or inclusions, lattice pitch, type of lattice, shape of holes. Some types of photonic crystal fibers are produced and commercially available and these include mainly silica glass based PCFs or PBGs. Various compositions of soft glasses, combining hyperspectral transmission windows with high nonlinearity or thermal and rheological properties enabling joint thermal processing into all-solid microstructured fiber optics enable demonstrating new structures covering new functionalities. All these components can be readily fabricated with the stack-and-draw (mosaic) method, provided good quality, recrystallization resistant glasses are used for preparing the starting elements (e.g. glass rods and tubes). Stack-and-draw at ITME was first used for fabrication of optic plates (FOP) in the '80, followed by fabrication of various specialty fibers e.g. for sensing [1, 2].

2. Stack and draw fabrication of microstructured fiber optics

The main concept of the stack-and-draw (mosaic) method is preparing a macroscopic element of a fiber optic element (i.e. fiber) by stacking glass rods (different shape – square, rectangular, round etc.), tubes, capillaries (different shapes), lightguide rods (different shapes) according to a predefined design. The obtained preform can be then drawn into microstructured integrated rods and finally into optical fibers (Fig. 1). The procedure of drawing stacked preform can be repeated until desired structure and dimensions of basic elements (diameters of fibers core, holes etc.) are achieved.

*e-mail: ryszard.buczynski@itme.edu.pl

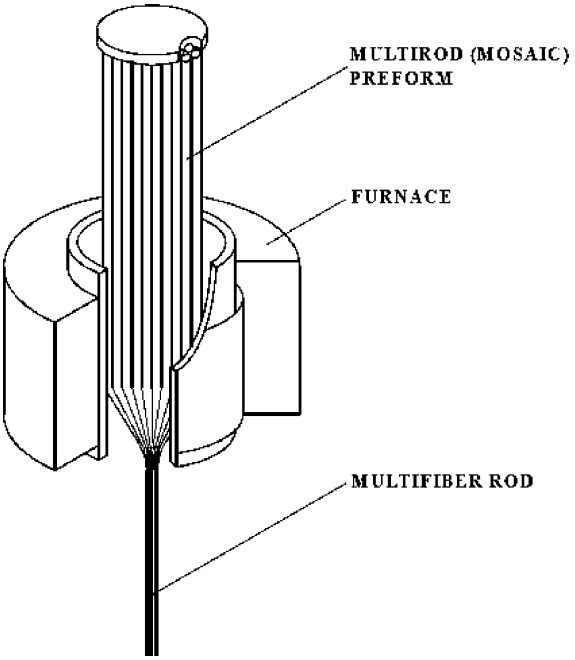

Fig. 1. Basic idea of a single drawing step in the stack-and-draw method of fabrication of microstructured fiber optic elements

The stack and draw procedure of microstructured optical elements (fibers) fabrication consists of a number of consecutive steps [2]:

1. melting of glasses – core, cladding, active, absorption glasses,
2. casting long rectangular prisms and thick-wall tubes,
3. cutting the glass blocks into rods (square, rectangular or round-shaped),
4. mechanical grinding and polishing of rods and tubes,
5. high temperature drawing of the rods, tubes, and stacked rod-in-tube preforms to standard dimensions of the mosaic elements,
6. assembling (stacking) of a preform of the designed structure, which may contain rods, capillaries and other elements. The preform can be assembled of elements of different dimensions and different refractive/mechanical/thermal properties. It can be arranged in a periodic lattice (PCF, image guide) or other structures (laser fibers, sensor fibers) as shown schematically in Fig. 2,
7. high temperature drawing of the stacked preform to obtain microstructured glass rod or optical fiber,
8. covering the fiber with a protective jacket (e.g. high index polymer for stripping of cladding modes in an optical fiber).

Fiber optic microstructures designed and fabricated at ITME are drawn mainly from multicomponent, soft glasses. Most of these glasses are designed and synthesized in-house. Multicomponent glasses enable broad flexibility in shaping of refractive index properties (n_D = 1.48–1.85); thermal, mechanical, chemical properties; preparing active elements (rare earth ion doped phosphate, fluoride glasses), manufacturing elements of preforms (rods of different shape, tubes). An important enabler of owning the glass synthesis capability is thermal matching of glasses with different refractive index profiles. This allows for fabrication of special, all-solid glass photonic crystal fibers and fiber optic elements, briefly discussed in one of the following sections of this review.

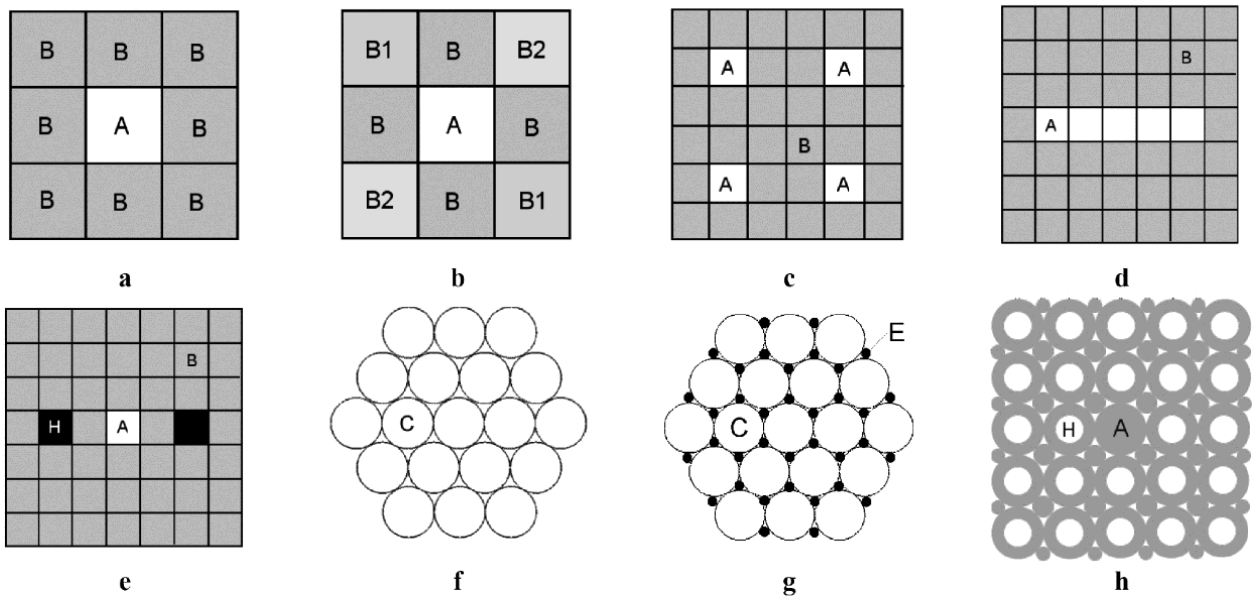

Fig. 2. Schematic examples of different stacked fiber optic structures: a–e lightguide, sensor structures (A – core glass, B, B1, B2 – different property cladding glasses, H – hole) [2]; f, g image guide structures (C – lightguide rods, E – EMA glass), h – photonic structure (A – core glass, H – hole)

3. Microstructured image guides

A fiber optic image guide is an arranged bundle of small diameter lightguides (2.5–50 μm). It allows to transmit image due its coherent structure and low attenuation of the individual fibers. The bundle is thermally integrated and preserves its coherence over the whole length. The smaller is the diameter of single individual fiber and greater their total number, the better is the guided image resolution. Figure 3 shows precision of transmitted image as a function of the resolution of the image guide structure.

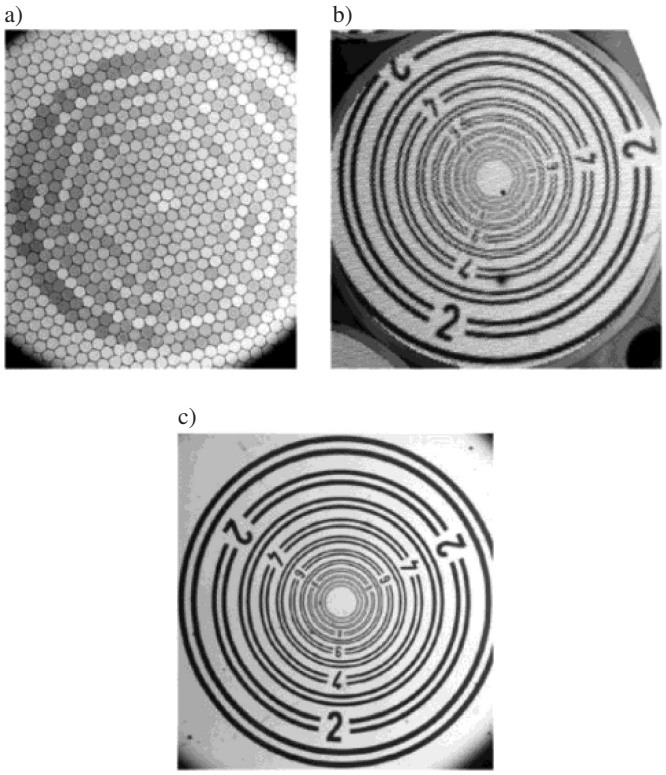

Fig. 3. Ring resolution test transmitted by different image guides. Size of pixels: a) 150 μm (fiber optic lightguide 2000 pixels), b) 18μm (image guide rod 12000 pixels), c) 5.5 μm (fiber optic plate, 100 pl/mm)

Depending on the transmission and structural parameters, the following fiber optic image guide structures can be distinguished:

1. **Light guide rods** – typically low resolution image guides with simpler technological procedure of fabrication, basic fibers with diameters of 100–200 μm, number of pixels 2000–3000, outer diameter 3–15 mm. Application in delivery of light, laser biostimulation devices, dental curing lamps. Fabrication – drawing from multirod preforms.
2. **Image guide rods** – medium and high resolution from 3000 to a several tens of thousands of pixels, basic fibers with diameter of 50–3 μm, outer diameter 0.5–10 mm. Applications in image delivery, technical and medical endoscopes, boreoscopes, industrial image conduits. Fabrication – drawing from multirod preforms, extra mural absorption (EMA) glass added to contrast enhancement.
3. **Fiber optic plates** – high resolution elements (50–200 pl/mm), basic fibers with diameters in the range of 10–2.5 μm, outer diameter of structure 15–50 mm, numerical aperture (NA) up to 1.0. Applications in image delivery, electronic image intensifiers (EII), night vision, cameras. Fabrication – two-stage multirod preform drawing, isostatic pressing.
4. **Fiber optic tapers** – high resolution 50–200 pl/mm, fibers with diameters of 10–2.5 μm, outer diameter 15–50 mm. Applications: image delivery with magnification or minimisation, interconnects between EII and CCD arrays, cameras, x-ray devices.

3.1. Fabrication. Preforms for drawing of image guide structures are made of arranged lightguiding rods. They form a periodic hexagonal (sometimes square) lattice of high index cores. Figure 2f,g shows fiber optic image guide structures. Difference between core and clad refractive indices influences the numerical aperture (NA) of the image guide. In case of FOP it can reach 1.0 which means 180° acceptance angle. To achieve such a large NA, special high index core glasses ($n_D = 1.85$, contents of lanthanum, tantalum, niobium) are necessary. In the large high resolution structures (FOP, tapers, some image guides) two stages of multirod preform drawing are necessary to achieve required diameters of basic fiber elements (3–5 μm).

The dark colored glass details seen in Fig. 2f in the structure of the image guide is added to increase contrast of the guided image. In the image guides with very small basic fibers (below 10 μm) the contrast of image tends to decrease (Fig. 4) [3]. For enhancement of image contrast a third, black glass which absorbs leakage light (EMA glass) is introduced in the structure during the preform assembly stage. Figure 5 shows typical designs with introduced details made from contrast enhancing glass.

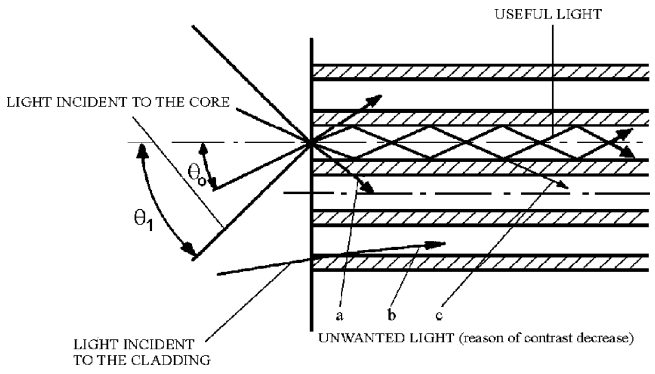

Fig. 4. Light propagation in the image guide. Phenomenon of decreasing contrast – light waves a,b,c [3]. a) Fibers acceptance angle (their numerical aperture) can be exceeded ($\theta_1 > \theta_0$, θ_0 – fibers acceptance angle), b) light guidance in fibers cladding, c) leakage of the light between adjacent fibers due their extremely thin (1–2 μm) cladding ("cross-talk" phenomenon) – occurs when diameter of individual fibers is about 10 μm or less

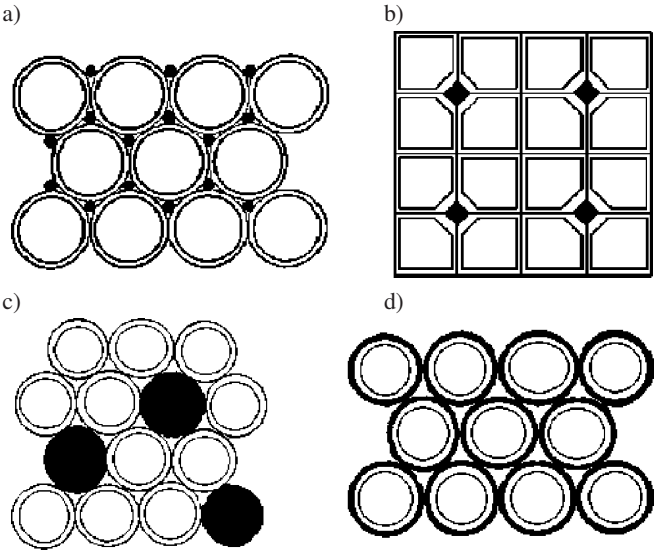

Fig. 5. Typical designs of image guide structures with introduced details made from contrast enhancing glass (seen in dark color)

All glasses – EMA, core, cladding must precisely match each other in terms of optical, thermal and rheological properties. Following criteria should be considered [4, 5]:

- refractive indices,
- thermal expansion coefficients,
- viscosity characteristic curves – thermal matching of glasses,
- inclination to diffusion of EMA glass to cladding,
- spectral transmission.

At ITME an EMA glass for contrast enhancement in integrated fiber optic image guides has been developed. It characterizes with low inclination to diffusion into glasses of the surrounding elements and it is well matched to core-clad glasses. These properties allow avoiding problems with appearance of dark and lower transmission pixels (Fig. 6). No degradations of the image guide structure, related to introduction of the EMA details, has been observed. (Fig. 7). Image guide with EMA glass details features better isolation of individual fiber cores, as seen in Fig. 7b.

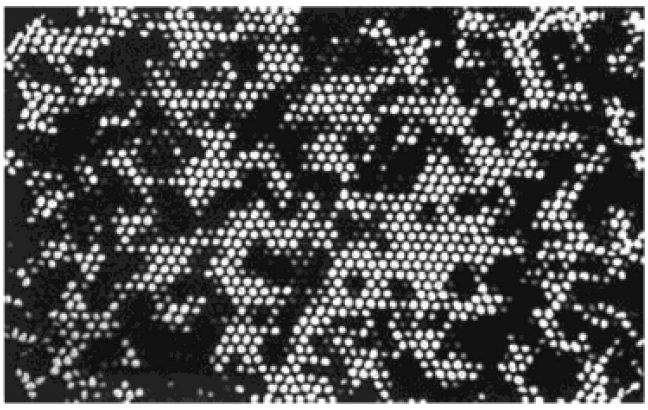

Fig. 6. Image guide structure containing EMA glass with high inclination to diffusion after Ref. 5

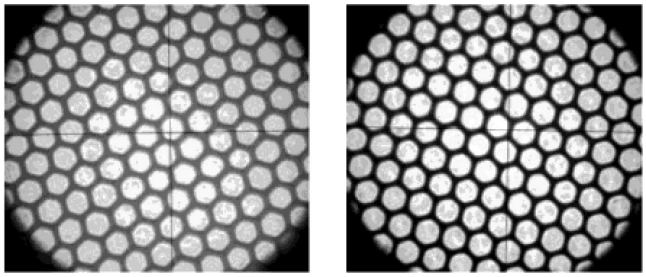

Fig. 7. Image guides cross section: a) without EMA glass, b) 1.5% contents of EMA ($\phi = 2.0$ mm, 16000 pixels)

Enhancement of the image contrast has been confirmed by measurements of the Modulation Transfer Function (MTF).

In Fig. 8 a comparison of image guides MTF in dependence on EMA glass contents is presented. Increase of contrast in the range of 0–40 pl/mm for image guides with EMA glass has been observed.

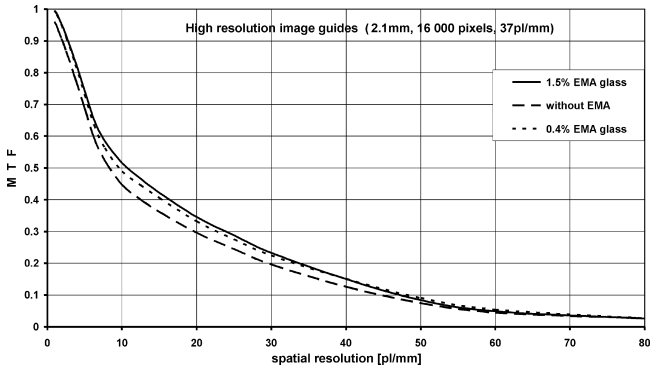

Fig. 8. Image guides MTF contrast dependence of EMA glass content

Table 1 summarizes properties of typical image guides manufactured at ITME.

Table 1
Technical parameters of the image guides fabricated at ITME

Outside diameter*	1.0–3.0 mm	
Length	up to 750 mm	
resolution	up to 16 000 pixels	
pixel diameter	10–20 μm	
Contrast** 10 pl/mm	50%	without EMA glass 45%
40 pl/mm	15%	without EMA glass 12%
Numerical aperture (NA)	0.52	
Absorption glass	up to 2% EMA glass; optionally	
Dark pixels	max 2%	
thermal resistance	up to 400°C	

* Square or rectangular cross sections are possible, depending on particular application.

** Measurements of modulation transfer function (MTF) at ITME.

4. Photonic crystal fibers

Photonic crystal fibers (PCFs, also called microstructured fibers) are optical fibers with an internal periodic structure of capillaries, typically filled with air, arranged in a lattice, eg. a hexagonal lattice. Light can propagate along the fiber

in defects of its crystal structure. A defect is realized by removing one or more central capillaries. Combining properties of classic, step-index optical fibers and photonic crystals they possess a series of unique properties impossible to achieve in classical fibers. There are two guiding mechanisms in PCF: index guiding mechanism (similar to the one in classical optical fibers) and the photonic bandgap mechanism. Figure 9 shows refractive index profiles of an index guiding PCF and bandgap guiding PCF (also called PBG). This lattice forms so called "photonic crystal" with lattice point diameter (d) in range of 0.5–5 μm and spacing (lattice constant Λ) 1–10 μm.

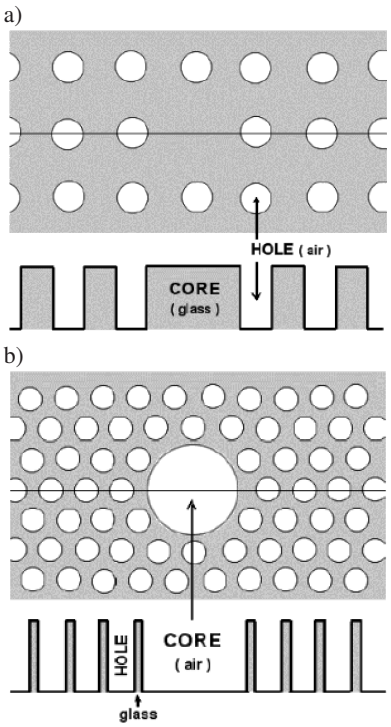

Fig. 9. Refractive index profile of PCF (a) and PGB fiber (b)

Stack and draw method enables designing and fabrication of a broad range of photonic crystal fibers. Preforms with different lattices – hexagonal, square, rectangular- and different ratio d/Λ can be considered. Presently, ITME can design and fabricate standard, as well as the more complicated microstructures (e.g. multicore, noncircular holes, different sizes of holes, and with additional different glass microfibers, laser fibers with air cladding). Photonic crystal fibers presented in the following section from various oxide soft glasses. Their attenuation is relatively high, in the range of several to about 15 dB/m. At this level, it is about 1000 times higher than in telecommunication silica fibers, but it is not disadvantageous for short lengths of fibers used, e.g. in sensors or active elements. The multicomponent soft glasses can accept much higher dopant concentrations and therefore the range of possible modifications of their optical and mechanical characteristics is much wider than in the case of silica glass. They also enable fabrication of more complicated microstructures due to e.g. joint thermal processing of a structure comprising two thermally matched glasses with a refractive index difference. Designing of photonic crystal fibers presented in this review was done at the Information Optics Group of Faculty of Physics at University of Warsaw. In the simulations a full vector method of biorthonormal basis, derived from the works of Silvestre *et al*. [6–8], has been used, where a matrix representation of the vector wave equations is calculated on the basis of plane waves and an eigenvalue problem is solved for that matrix. The vector wave equations involve a pair of Hermitian-conjugate operators whose eigenvectors satisfy the bi-orthonormality relations.

4.1. Stack and draw fabrication of photonic crystal fibers. Stack-and-draw fabrication of photonic crystal fibers consists typically of the following main stages:

1. Drawing of the basic preform elements: glass capillaries, rods, tubes – Fig. 10a.
2. Stacking of macroscopic mosaic preform according to the designed structure; at this stage the type of lattice, hole/spacing ratio, distribution of capillaries, rods, etc., is decided, introduction of special elements for specific properties (active, sensing, conductive, magnetostrictive, etc.) should also be done now – Fig. 10b.
3. Intermediate preform (subpreform) drawing. Structure of the subpreform resembles the designed photonic crystal fiber, but its geometric dimensions are at the order of several mm – Fig. 10c.
4. Arrangement of the preform for fiber drawing. Adding outer layers of glass to achieve designed dimensions of the fiber (photonic structure/fiber diameter ratio).
5. Drawing of photonic crystal fiber. At this stage parameters like air-holes diameter, relative air-hole size and fiber diameter can be influenced through the parameters of drawing process (temperature, preform feeding rate and drawing speeds) – Fig. 10d.

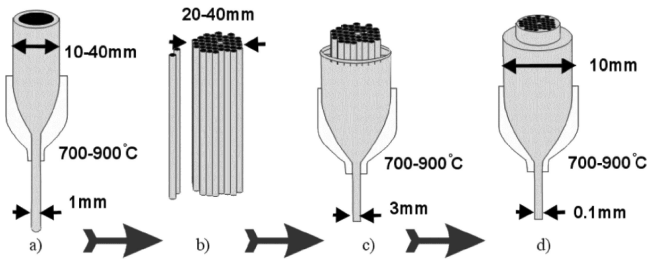

Fig. 10. Photonic crystal fiber fabrication: a) creation of individual capillaries; b) perform formation; c) drawing of intermediate preform; d) drawing a the final fiber after Ref. 9

Stages 2 and 5 are decisive on the resulting fiber optical properties and thus are usually considered most critical.

4.2. Square and hexagonal lattice single core photonic crystal fibers. Single core PCF can be considered the simplest design of a microstructured fiber. Its structure consists of a solid core surrounded by periodic lattice of air-holes. Diameter of air-holes, lattice pitch and relative hole size (the

ratio of holes diameter to lattice constant) decide about guiding properties of the fiber. A series of hexagonal and square lattice single core PCFs have been designed and successfully fabricated in our group. Schematic designs and images of the drawn subpreforms and final fibers are presented in Fig. 11. It is notable how precisely the fiber and subpreform reproduce the design of the preform structure. The stage of preform stacking is very important for the whole technological process. At this phase it is possible to change the type of lattice core dimensions, the number of capillary rings around the core, the relative hole size etc. Parameters of the preform's basic elements and the way the preform is stacked, determines the final fiber's geometrical and transmission properties. For example, in hexagonal lattice fiber A in Fig. 11, one central capillary has been replaced with a glass rod to form a core, in fiber B (Fig. 11) 7 central rods form the core of a Large Mode Area fiber (LMA). Fiber C in Fig. 11 has a square photonic lattice, which was selected to achieve new dispersion properties (in comparison to most popular, hexagonal lattices). In our technological process, the subpreforms typically are 2–4 mm in diameter. The standard diameter for an optical fibers is 125 μm, but different diamerters are possible to fabricate, in order to obtained the desired properties of the final fiber. The outer diameter of fiber C in Fig. 11 was 180–200 μm with a lattice constant of 2.3 μm and relative hole size of about 0.2, in order to maintain single fundamental mode guidance.

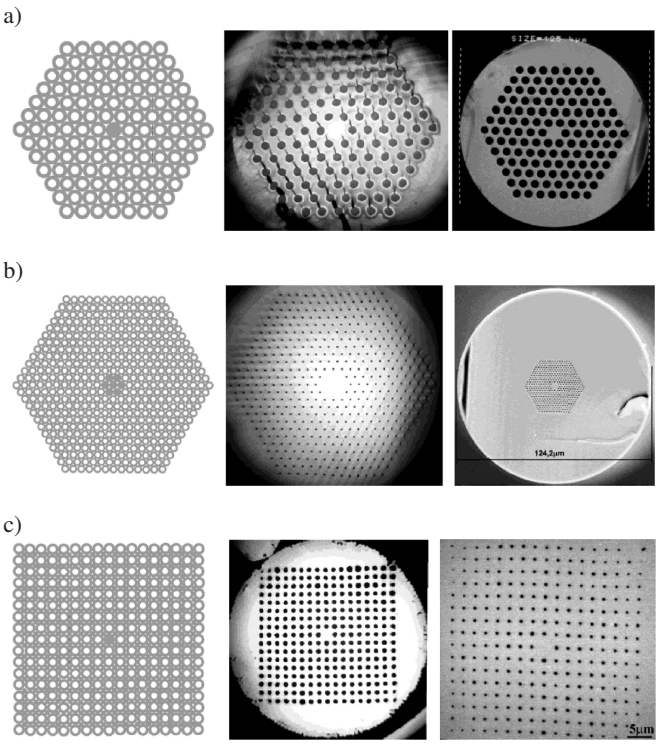

Fig. 11. Single core PCF fibers (left to right: design of photonic structure, SEM image of subpreform, SEM image of the final fiber); a) hexagonal lattice multimode PCF; b) hexagonal lattice, large mode area PCF; c) square lattice, single mode PCF

Light propagation in the different single core PCFs is shown in Fig. 12. Single mode transmission has been observed in the fibers B and C. Fiber A is multimode due a rather high relative hole size of 0.65. Attenuation of soft glass photonic crystal fibers can be in range from one to several dB/m and depends on the type of glass, its purity, type of photonic structure, its parameters and presence of defects. For example fiber A (Figs. 11, 12) had a measured attenuation about 15 dB/m at 632 nm. It seems high but it was close the attenuation of used glass, due to perfect photonic crystal structure obtained during drawing (the drawing process itself did not introduce additional loss). The fiber A in Fig. 11 and 12 was drawn from heavy metal, lead-bismuth-gallate oxide glass (designated PBG-08), which has a high refractive index (1.95) and strong nonlinear properties, while its transmission window extends from the visible up to about 4–5 μm. This fiber has been successfully used in developing of a liquid crystal PCF by the group of T. Woliński at Warsaw University of Technology [10].

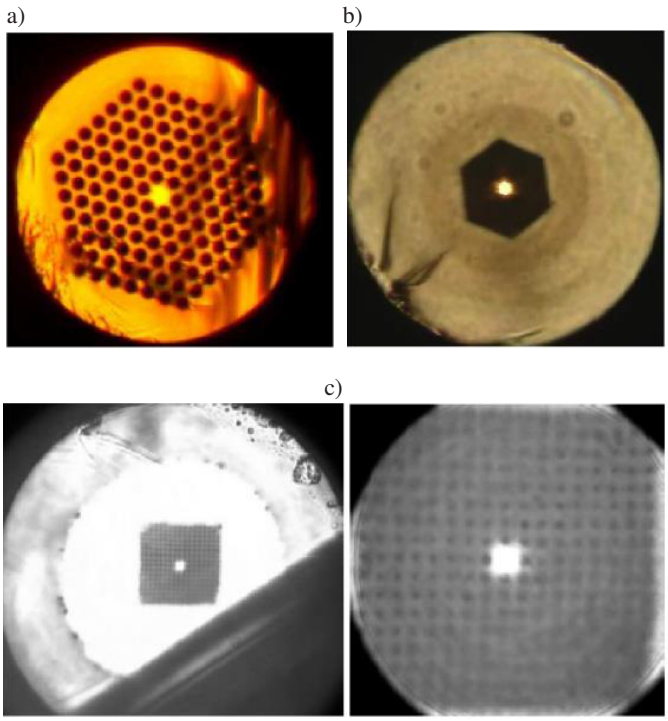

Fig. 12. Light guidance in the single core different lattice PCFs fabricated in ITME

4.3. Double core photonic crystal fibers. The stack and draw method enables straightforward fabrication of multicore PCFs by replacing proper number of capillaries with glass rods. Furthermore, the procedure allows for very precise positioning of the cores in the structure. Dimensions of the cores and distances between them can vary in wide range by design [11]. Double core PCFs at ITME were investigated in context of controlling the light coupling between the cores. Possible applications are directional couplers, wavelength multiplexers/demultiplexers and bend sensors, for example [12]. Preform desing and cross sections of square lattice double core subpreforms and PCFs are presented in Fig. 13.

The photonic structure contain two solid cores formed by replacing of capillaries by glass rods. The cores were separated with one capillary. Figure 13 presents possibility to change inner hole diameter at the stage of subpreform drawing. Different inner diameters of the central capillary were investigated to achieve the effect of variable inter-core coupling [13]. A double-core PCF arranged in a square pattern lattice has been successfully drawn with outer diameter of 220 μm. Figure 14 shows the cross-sections of the final square lattice PCF with different lattice parameters as well as a hexagonal lattice double core PCF.

For the square lattice double-core PCF we determined linear optical properties of the fiber by numerical simulations assuming a perfect structure (no deformations). Only the fundamental mode can propagate in either of the cores. Pairs of polarization components are nearly degenerated for $\lambda = 1.55$ μm and their mode indices are equal to 1.5497 and 1.5462 for even and odd modes, respectively. It can be concluded that in the fabricated structure coupling lengths are almost equal for both orthogonal polarizations, as summarized in Table 2. The coupling lengths were estimated at 221 μm. Only the fundamental mode without higher order components was also observed experimentally. The attenuation of the fabricated PCF was 15 dB/m for the wavelength of $\lambda = 632$ nm and 7 dB/m for $\lambda = 1.55$ μm [13].

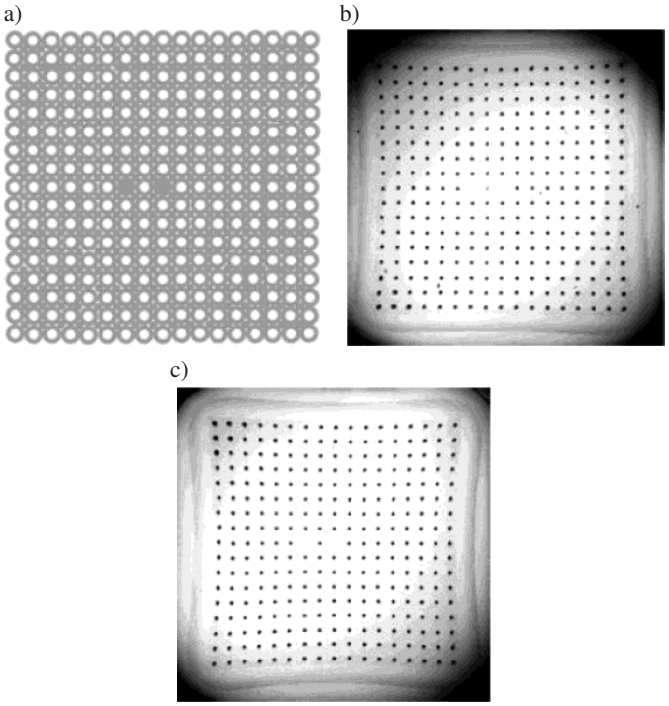

Fig. 13. Double core square lattice PCF: a) project of preform, b),c) subpreforms with different size of the air-hole separating the cores

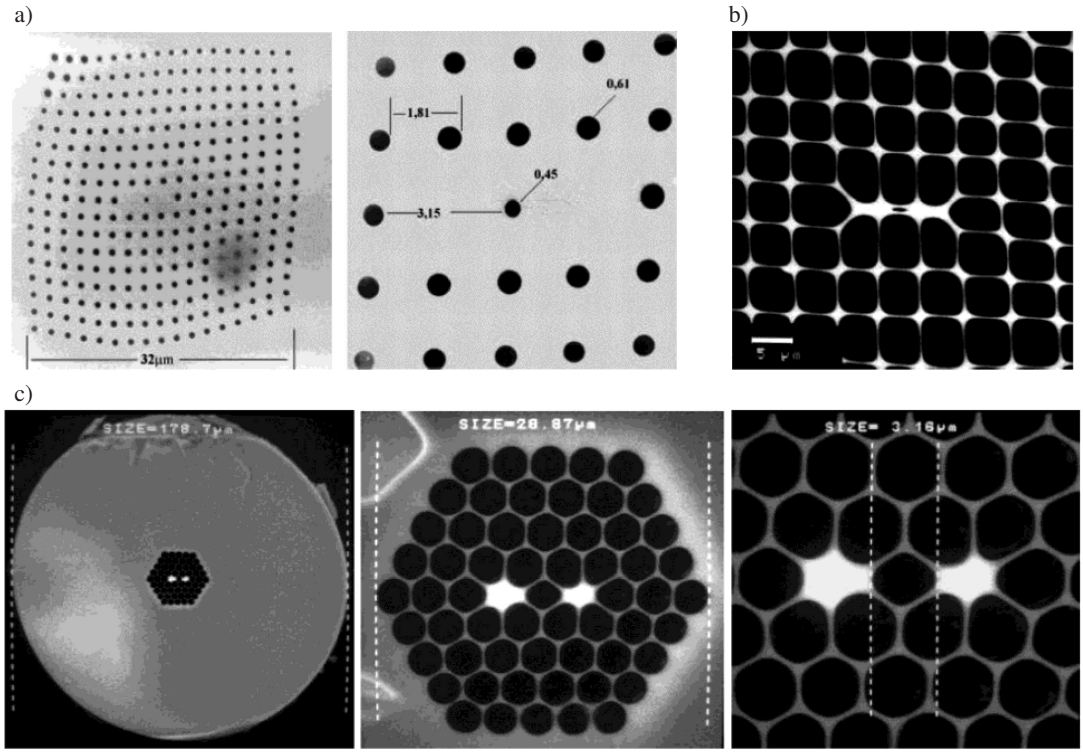

Fig. 14. The structure of a double-core PCF fibers: a) with a square lattice, fiber's diameter of 220 μm, lattice constant $\Lambda = 1.81$, the hole diameter $d = 0.61$ μm ($d/\Lambda = 0.34$), central hole diameter $d_c = 0.45$ μm after Ref. 13; b) square lattice with modified structure (high filling factor); c) with heksagonal lattice, fiber's diameter 179 μm, the hole diameter $d = 3.4$ μm ($d/\Lambda = 0.94$), central hole diameter $d_c = 3.2$ μm (SEM)

Table 2
Mode indices and coupling lengths for a structure with $\Lambda = 1.81$ μm, $d = 0.61$ μm, $d_c = 0.45$ μm, $\lambda = 1.55$ μm after Ref. 13

	$n_{even,x}$	$n_{even,y}$	$n_{odd,x}$	$n_{odd,y}$	L_x	L_y
for $\lambda = 0.63$ μm	1.5656	1.5656	1.5652	1.5651	692.0 μm	701.7 μm
for $\lambda = 1.55$ μm	1.5497	1.5496	1.5462	1.5462	220.5 μm	221.2 μm

4.4. Highly birefringent photonic crystal fibers. High contrast of refractive index and high freedom of crystal structure modification allow to achieve in the PCF a birefringence in a level of 10^{-2}–10^{-3}. It is above one order of magnitude greater, than in classical (*bow tie* and *panda* type) birefringent optical fibers. So high level of birefringence is possible in the structures of elliptical holes and refractive index distribution with symmetry $m = 2$ (rectangular lattice) [14, 15].

We have decided to manufacture such a fiber in form of rectangular lattice with elliptical or round holes. Choice of rectangular lattice is motivated by possibility of birefringence value increase by crystal lattice anisotropy and asymmetry of holes shape. A range of PCFs with rectangular 9×9 holes structure has been manufactured from silicate glass ($n_D = 1.52$). Photonic structures of these fibers are presented in Fig. 15. Lattice pitch in different axes is: $\Lambda_x = 2.89$ μm, $\Lambda_y = 3.64$ μm and round holes of 2.0 μm in diameter (Fig. 15a,b). In other fibers the elliptical holes 0.57×1.2 μm have been achieved (Fig. 18c). Dimensions of fiber are 134×200 μm.

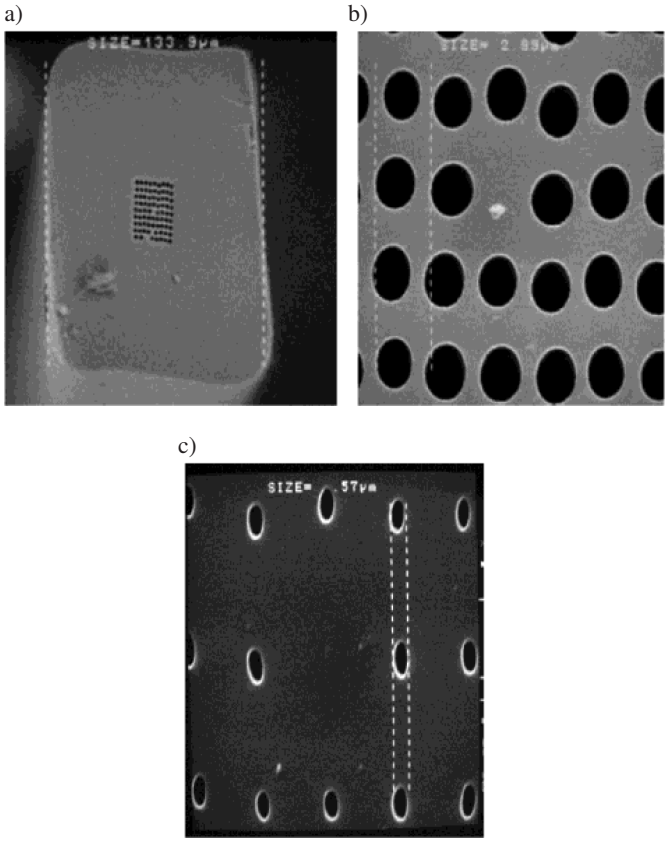

Fig. 15. Highly birefringent PCF with rectangular lattice and round (a,b), or eliptical (c) holes

This structure predicts fiber witha high birefringence. Simulations of rectangular structure with the parameters $\Lambda_x = 1.24$ μm, $\Lambda_y = 0.96$ μm, $l_x = 1$ μm, $l_y = 0.51$ μm have shown birefringence $B = 1.1 \times 10^{-2}$ and the fiber carries only the fundamental mode [15]. In Fig. 16 a different structure of highly birefringent PCF manufactured in ITME is presented. Birefringence is achieved here by different sizes of holes surrounding core and its rectangular shape.

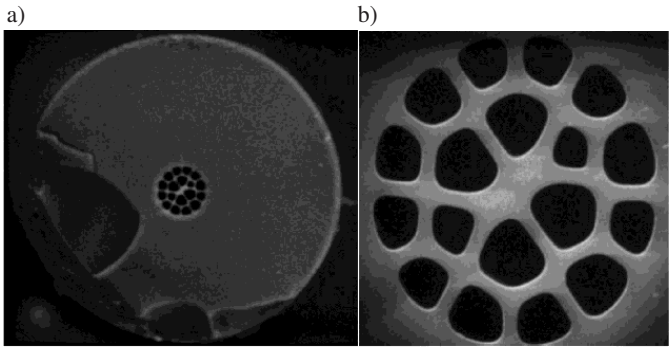

Fig. 16. Hexagonal lattice highly birefringent PCF (SEM image)

Modeling of highly birefringent photonic fibers and propagation properties have been presented in the paper nr 5950-58 on this Congress on Photonic Crystals and Fibers Conference [16].

4.5. Photonic bandgap fibers. One of the most interesting properties of photonic fibers is the possibility to build structures which can guide light in the core with lower refractive index (hollow or solid). Mechanism of propagation in this case is existence of a photonic band gap in a photonic crystal and possibility of light being trapped in the defect – hollow core (a few lattice constants in diameter). Since in a large core most of energy is transmitted in the air, all effects related to interaction between glass and light (Rayleigh scattering, dispersion, nonlinear effects) are strongly reduced. Such fibers are expected to achieve ultra-low transmission losses.

Hollow core PBG fibers. Microstructured PBG fibers with a square or hexagonal lattice (using a silicate glass with $n_D = 1.52$) were developed at ITME with the objective to verify the possibility of achieving the PBG effect in a multicomponent glass photonic fiber and to check its guiding properties. Figure 17 shows the designed structures of the preforms, the cross section of the drawn subpreforms and the final fibers for square and hexagonal lattice hollow core fibers. In the structure of the square lattice PBG fiber a total of nine (3×3) capillaries were removed to achieve 11 μm hollow core in a 125 μm fiber. Fiber in Fig. 20b has a hexagonal lattice with

a relatively large (31 μm) hollow core created by removal of 37 central capillaries. The fiber C is a double hollow core. Cores are separated by one hole structure. Each has 18 μm in diameter (in a 117 μm fiber) and were formed by removing of 19 for each core. All PBG fibers presented in Fig. 20 have very high relative air hole size (d/Λ) which is necessary for existence of a photonic bandgap.

Figure 18 shows measured transmission spectrum of a square lattice PBG fiber shown in Fig. 17a. Obtained results revealed existence of a bandgap at about 1600–1700 nm (which was already close to the long-wavelength sensitivity limit of the OSA). We measured the transmission for several lengths of the fiber (Fig. 18). An increase of the bandgap size for shorter pieces of the fiber was observed as expected.

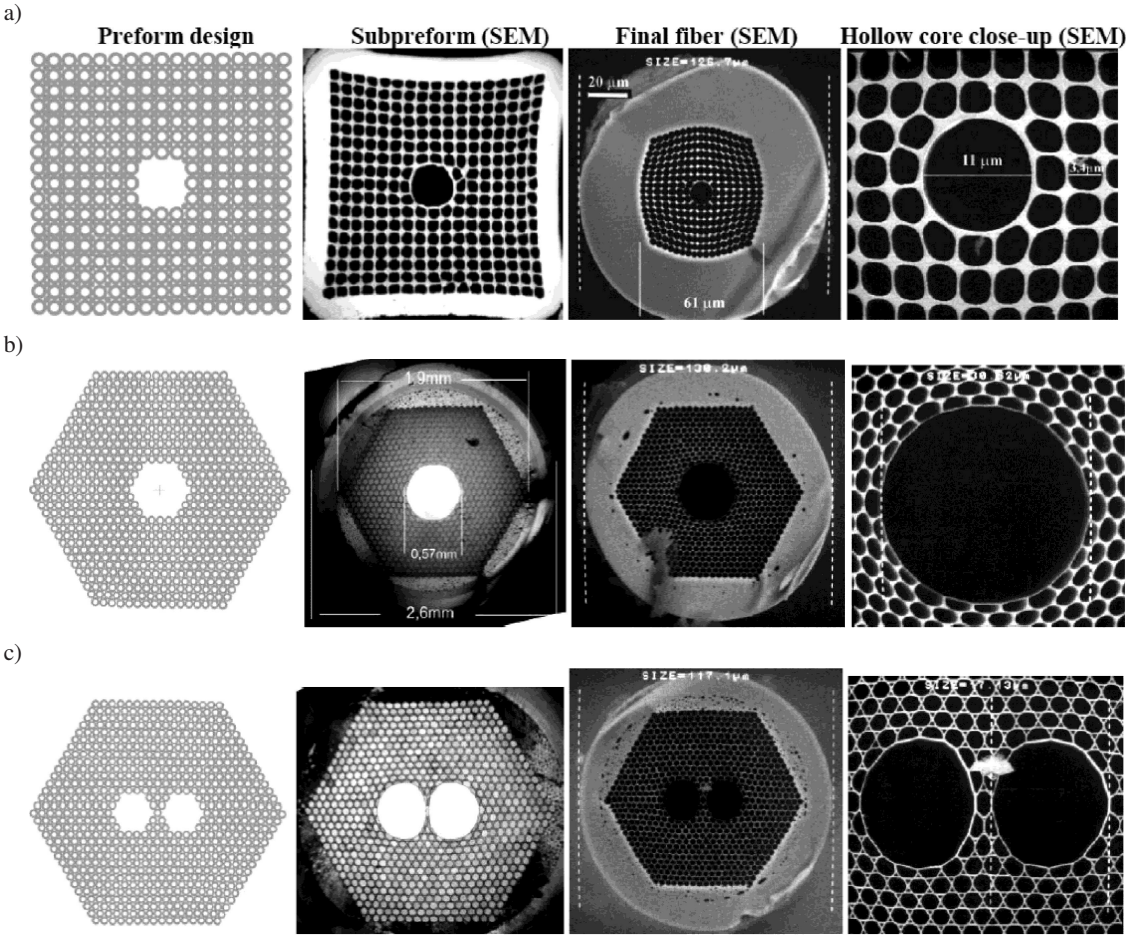

Fig. 17. Hollow core PBG fibers: a) square lattice single core (fiber diameter 125 μm, lattice constant 3.6 μm, $d/\Lambda = 0.94$, core diameter 11 μm); b) hexagonal lattice single core (fiber diameter 130 μm, lattice constant 3 μm, $d/\Lambda = 0.93$, core diameter 31 μm); c) hexagonal lattice double core (fiber diameter 117 μm, lattice constant 2.9 μm, $d/\Lambda = 0.93$, diameter of each core 18 μm)

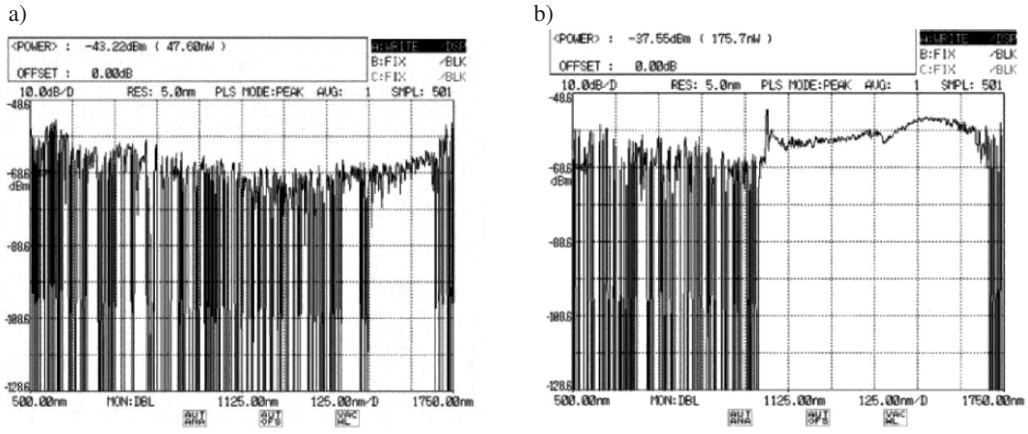

Fig. 18. Transmission of white light through 115 μm square lattice hollow core PCF, for a sample a) 50 cm long and b) 30 cm long after Ref. 17

Images demonstrating propagation of light in the hexagonal lattice hollow-core PBG fibers are presented in Fig. 19. For the single hollow core fiber (Fig. 17b, Fig. 19a) photonic bandgap existance and guidence of light in range 560–670 nm is clearly observable. Measurements of transmission for the fiber B (shown in Fig. 17b, length 103 cm) are presented in Fig. 20. Measured attenuation of this fiber was 2.1 dB/m what is far below glass attenuation (about 15 dB/m). In the case of double hollow core fiber (Figs. 17c, 19b) a wide, photonic bandgap exists in the range of 595–750 nm. Transmission measurements for each core individually are shown in Fig. 21 [18]. Figure 19c shows propagation of green light (incident light was white) in a hollow core of a 235 μm PBG fiber. Central air-hole diameter is 16 μm, structure air-hole diameters are 5.5 μm, relative hole size is for this fiber is $d/\Lambda = 0.9$. Details of designing of these fibers and related numerical modeling was summarized in [17].

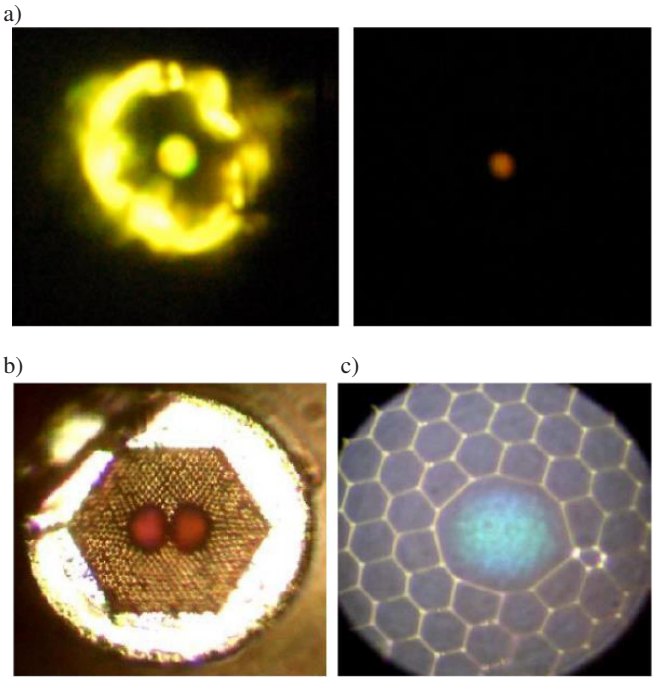

Fig. 19. Hexagonal lattice hollow core PCFs. Guidance of light in the hollow core in the wavelength range of the photonic bandgaps can be observed

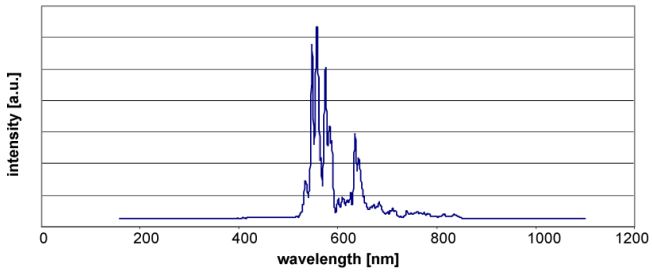

Fig. 20. Spectrum transmitted by hollow core of hexagonal lattice PBG fiber (outer diameter 130 μm, lattice constant 3 μm, $d/\Lambda = 0.93$, core diameter 31 μm, sample length 103 cm)

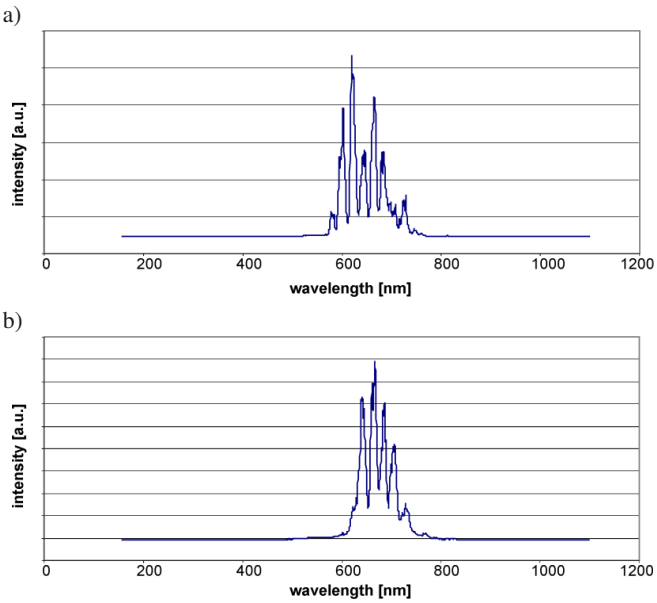

Fig. 21. Spectrum transmitted by left (a) and right (b) hollow core of double core PBG fiber (outer diameter 117 μm, lattice constant 2.9 μm, $d/\Lambda = 0.93$, cores diameter 18 μm, length 87 cm)

Solid core (all glass) PBG fibers. Several designs of all-glass PBG fibers have been developed and fabricated at ITME. Figure 22 presents a selected example of a solid core PBG fiber fabricated at our Institute. The fiber was drawn from two glasses: F2 (Schott) as the high index (1.62) and NC21 (ITME melted) as the low index (1.53) glass. Core was created by 7 rods of the low index glass.

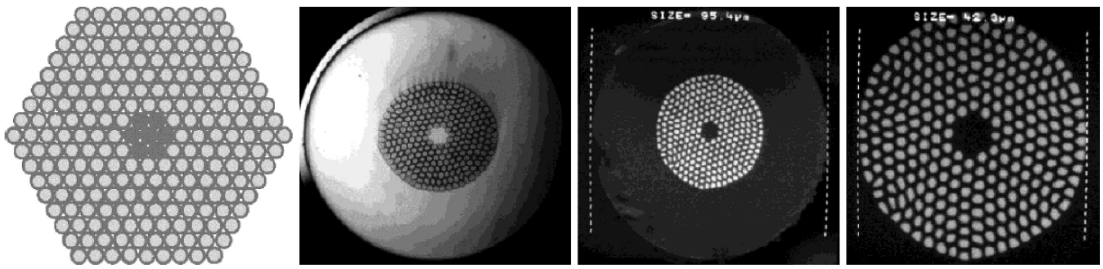

Fig. 22. Solid core (all-glass) PBG fiber, from left to right: preform design, subpreform, image of fiber, close-up of the photonic structure; final fiber dimensions: diameter 95 μm, lattice constant 2.5 μm, $d/\Lambda = 0.65$, core diameter 8 μm

Figure 23 shows propagation of white light in this fiber and corresponding transmission spectrum, reveals two photonic bandgaps: one 9 nm wide with central wavelength at 610 nm and second 80 nm wide centered at a wavelength of 860 nm (Fig. 24). Attenuation of this fiber was 13.3 dB/m measured for $\lambda = 835$ nm (core glass attenuation was 8.2 dB/m) [19].

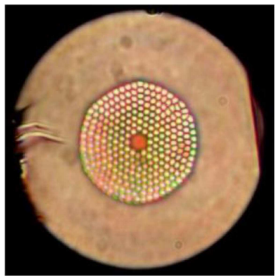

Fig. 23. Solid core (all-glass) PBG fiber and light propagating in its core made from lower index glass (guidance due to photonic bandgap effect)

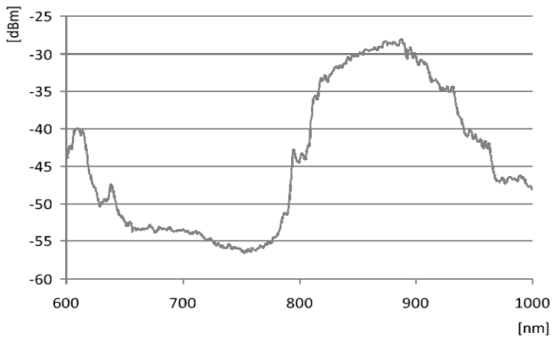

Fig. 24. Spectrum transmitted by the solid core all-glass PBG fiber (fiber length 18.5 cm)

4.6. Photonic crystal fibers with double lattice (air holes and microfibers). Stack-and-draw method allows fabrication of soft glass photonic crystal fibers with more complicated designs, than summarized in previous sections. A double-lattice PCF was proposed in [20], which consisted of a lattice of air-holes with superimposed lattice formed by inclusions from a second, higher-index glass. Introduction of such inclusions required the second glass to be thermally matched to the main glass forming the fiber's structure. Joint thermal processing of two-glass structure opens up new possibilities in designing of optical properties of a PCF and will be discussed in more detail in a following section of this paper.

Design and subpreform of the PCF proposed in [20] is shown in Fig. 25. It had a 17×17 square air-hole lattice, with a superimposed lattice of 16x16 inclusions and a solid central core, obtained by replacement of one capillary with a glass rod. Additional glass rods with $n_D = 1.619$ (Schott's F2 glass) and diameter adjusted to obtain 300–400 nm diameter in the final fiber, were used. Refractive index of the primary glass of fiber's structure was $n_D = 1.518$ (in-house synthesized glass). The final fiber is shown in SEM images in Fig. 26. Fiber diameter was about 140 μm, lattice constant 2.2 μm, diameter of air-holes was 1.4 μm, core diameter 3 μm, diameters of inclusions was 320 nm. Lattice of inclusions can be observed in the SEM in Fig. 26. The photonic structure has only small deformations but they are located away from the fiber's central area with the core, Fig. 26. The defect seen in Fig. 25 do not influence global guiding properties of the fiber. Guiding of white light was recorded experimentally in this fiber together with selective (red to blue depend on fiber's diameter) guiding in microfibers. Also a band gap effect has been identified in the fiber containing only microfibers square lattice, Fig. 27. Another PCF with hollow core has been designed as square, 17×17 air-hole lattice with a superimposed 16x16 solid inclusion lattice (inclusions located between capillaries). Refractive index of inclusions was $n_D = 1.609$ (zirconium silicate glass, synthesized at ITME). The primary glass was a sodium-calcium silicate glass with $n_D = 1.52$. Hollow core was arranged by removal 9 (3×3) capillaries. Structure design, drawn subpreform and an image with close-up of its structure with visible inclusions is presented in Fig. 28.

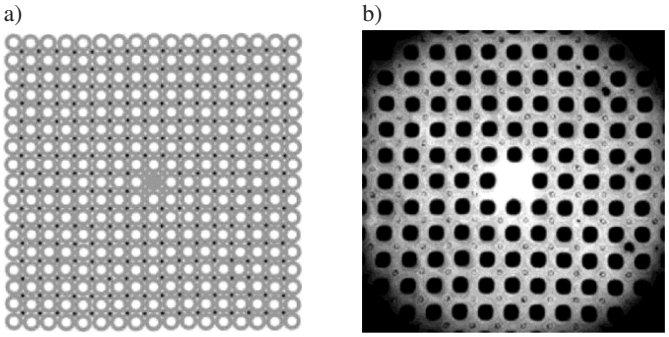

Fig. 25. PCF with double, square lattice (air holes and solid inclusions): a) structure design; b) actual subpreform cross section (diameter 6.25 mm)

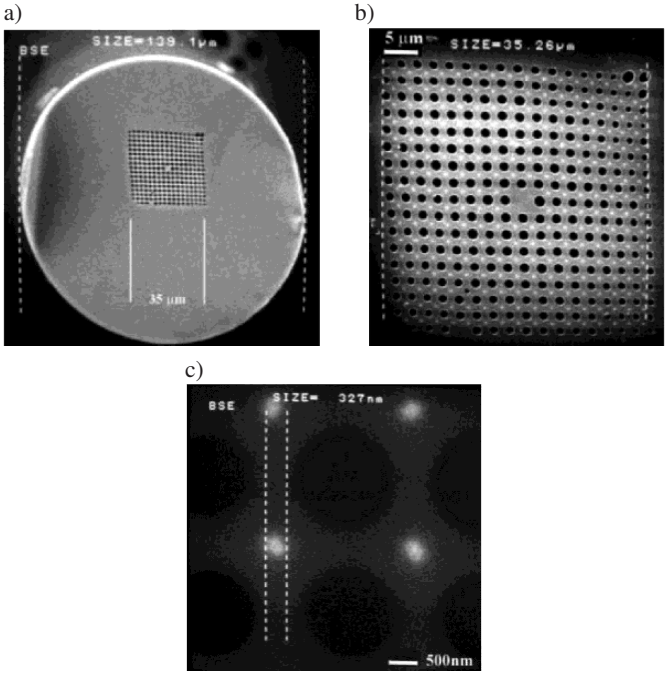

Fig. 26. PCF with double, square lattice (holes and microfibers) (SEM)

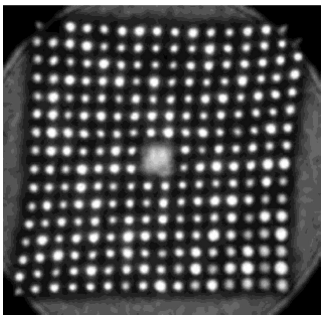

Fig. 27. PBG effect in the fiber with square lattice of microfibers made from higher refractive index glass

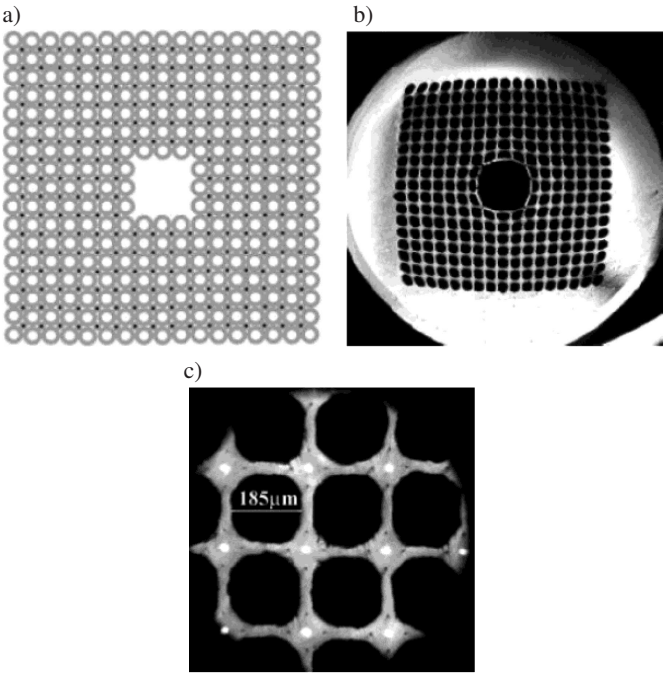

Fig. 28. Hollow core PCF with double square lattice consisting of air-holes and solid inclusions: a) design of photonic structure; b), c) sub-preform cross sections

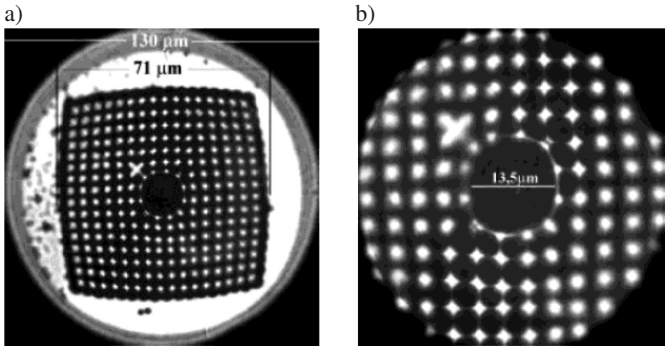

Fig. 29. Hollow core PCF with double (holes and microfibers) square lattice

4.7. Highly nonlinear single-mode photonic crystal fibers for supercontinuum generation. Supercontinuum generation (SG), first reported in the '70 [21], has been extensively studied in the past decade in context of photonic crystal fibers. PCFs enable unique advantages for SG in terms of dispersion engineering, so that the dispersion profile of the fiber, critical to efficiency of the nonlinear broadening process, can be used to fabricate PCFs with zero-dispersion wavelength matched to highly efficient laser pump sources [22]. Of particular interest in the recent years are glasses which enable mid-infrared transmission – SG up to around 4–5 μm has been reported eg. tellurite glass suspended core photonic crystal fiber [23], chalcogenide glass fiber [24] and various fluoride step-index fibers [25].

Our group develops nonlinear PCFs from heavy metal oxide glasses of the TeO_2-WO_3-(Na_2O+Nb_2O_5) and SiO_2-PbO-Bi_2O_3-Ga_2O_3-CdO systems (designated TWPN/I/6 and PBG-08 respectively). Both glasses combine advantages of broad transmission window from the visible to the mid-infrared around 5 μm, high value of nonlinear refractive index n_2 and high resistance to recrystallization. Transmittance spectra of both glass systems are shown in Fig. 30 together with one of Schott's soft glasses characteristic for reference. Recently three PCFs designs were demonstrated, which enabled SG covering the entire near-infrared spectrum up to around 2.5–2.7 μm. Presently, onset of OH absorption at around 2.8 μm prohibits further redshift of spectra. Since this is not the multiphonon absorption edge of these glasses, enhancements in glass synthesis technology should enable to overcome this problem.

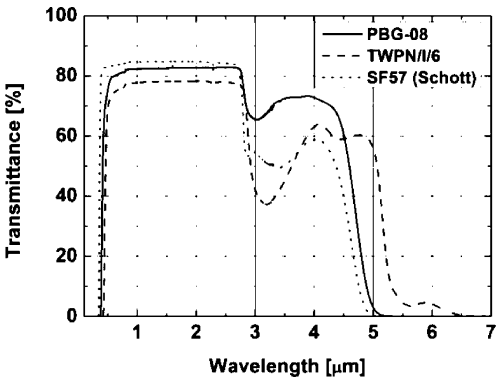

Fig. 30. Transmittance spectra of TWPN/I/6 and PBG-08 soft glasses with Schott's SF57 glass for reference

Two PCFs were designed with a regular, hexagonal lattice of air-holes and one with suspended core lattice. The first fiber, drawn from tellurite glass TWPN/I/6, is shown with guided mode in Fig. 31a. It has 120 μm outer diameter. The hexagonal photonic structure is 23 μm in diagonal, the lattice constant is $\Lambda = 2$ μm, linear filling factor $d/\Lambda = 0.75$ μm, and a solid core has 2.7 μm diameter. Fiber core has a very regular, circular geometry, which should result in negligible birefringence. Calculated birefringence of this fiber was below 10^{-6}. Dispersion profile of the fiber shown in Fig. 31b, calculated from SEM image of the drawn fiber, has ZDW at 1410 nm and 4236 nm with a maximum of 193 ps/nm/km at 2800 nm. Calculated effective mode area at pump wavelength was 3.0 μm^2. For a measured nonlinear refractive index of our glass $n_2 = 18 \times 10$–20 m^2/W, this value yields non-

linear coefficient $\gamma = 238.6$ W^{-1}km^{-1}. SG in this type of PCF was obtained under pumping with 150 fs pulses centered at 1580 nm. Experimentally recorded supercontinuum spectra for incident pump pulse energies of 15, 25 and 35 nJ are shown in Fig. 31c. The measured spectra were stable and fluctuated only with input laser intensity variations. All spectra were recorded in only 2 cm long PCF sample [26]. The second fiber was drawn from the PBG-08 glass and had a suspended core photonic structure, in which the central core (1.2 μm id diameter) area was surrounded by three large air-holes, as shown in SEM images in Fig. 32a. Thickness of the supporting struts was about 290 nm. Dispersion profile, calculated for the fiber using real fiber structure revealed zero dispersion wavelength located over 1600 nm, which precluded efficient pumping on the anomalous side of the ZDW with disposed pump sources operating at around 1550 nm. Nevertheless, experimentally recorded supercontinuum spectrum – shown in Fig. 32b – under pumping with 70 fs pulses at 1550 nm reached a wavelength of 2600 nm for fiber sample length of just 5.5 cm [27].

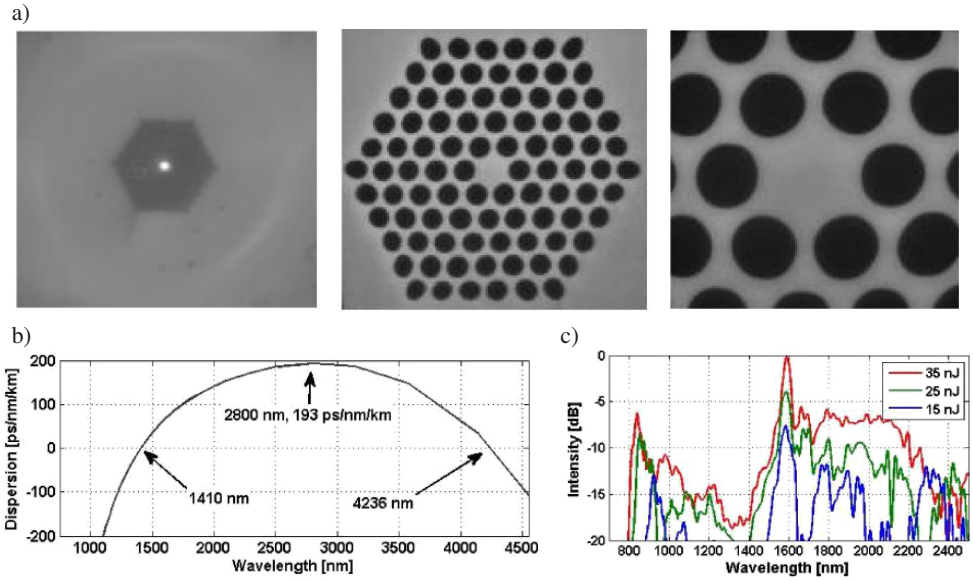

Fig. 31. a) Large image of photonic structure close-up with propagating mode as seen in a CCD camera, and SEM images of photonic structure, b) calculated dispersion profile of the PCF and C) measured supercontinuum spectra for incident pump pulse energy of 15, 25 and 35 nJ after Ref. 26

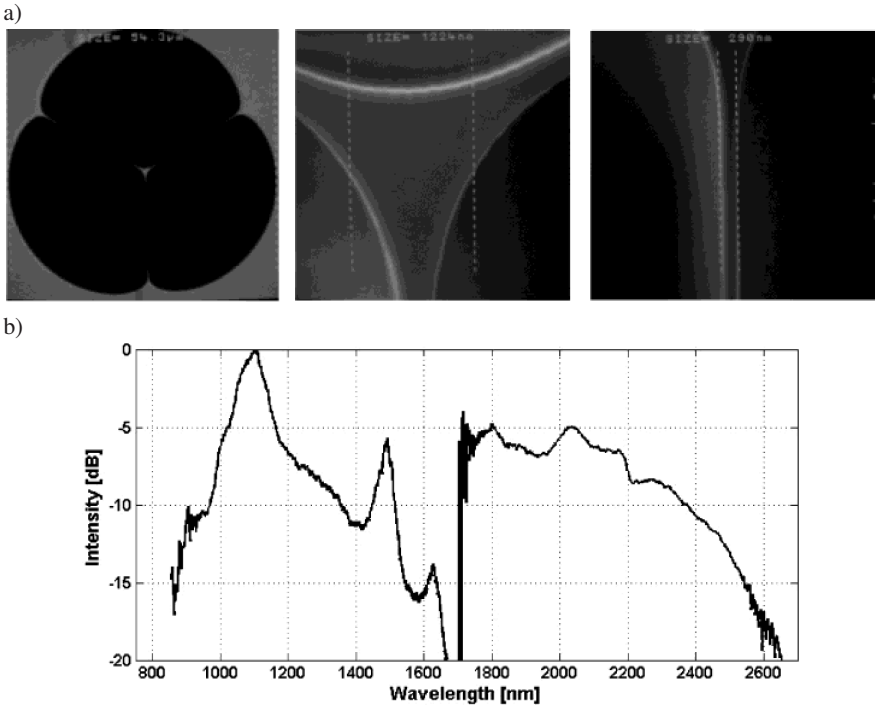

Fig. 32. a) SEM images of photonic structure of the developed suspended core photonic crystal fiber using PBG-08 glass and b) measured supercontinuum spectrum in the fiber [after Ref. 27]

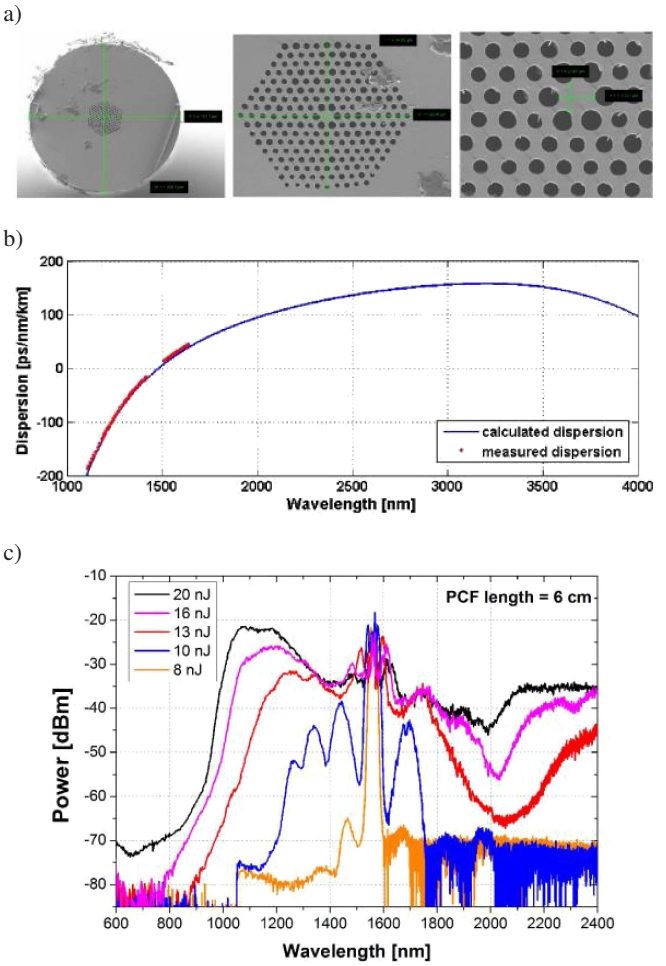

Fig. 33. a) SEM images of photonic structure with different relative air hole size b) calculated dispersion profile of the PCF and c) measured supercontinuum spectra for incident pump pulse energy from 8 to 20 nJ and pulse durations of about 0.9 ps from an erbium-doped, mode-locked fiber laser after Ref. 28

The third fiber, drawn also from PBG-08 glass, had a regular, hexagonal photonic crystal lattice, shown on SEM images in Fig. 33a. The lattice consisted of 8 rings of air holes with a lattice constant typically at $\Lambda = 2.4$ μm and relative hole size $d/\Lambda = 0.73$ in the first ring and $d/\Lambda = 0.5$ in the remaining seven rings. Relative hole size of the outer rings is decreased in order to increase modal losses of the higher order modes We verified numerically, that the fiber should be guiding the fundamental mode with negligible modal loss, and just a few higher order modes with significantly increased modal losses. We also measured near-filed output profile of the PCF, which was very close to pure Gaussian. Based on this, we consider the fiber to be effectively single mode. The diameter of the core of the PCF is 3.1 μm with a photonic cladding diameter of 39.4 μm. The total fiber diameter was 159.8 μm. Dispersion of the fiber was calculated using SEM image of the fiber structure and verified experimentally (unbalanced Mach-Zehnder interferometer setup) and location of zero dispersion wavelength was confirmed at around 1465 nm, Fig. 33b. As the pump source, a robust setup of an erbium fiber laser has been used, in which sub-ps pump pulses at 1550 nm were obtained by means of passive mode-locking with either nonlinear polarization rotator or graphene-based saturable absorber [28]. Supercontinuum spectra, shown for different input pulse energies in Fig. 33c, spanned the wavelength range from 800 nm to over 2400 nm, which was the limit of our measurement setup at that experiment.

4.8. All-solid glass photonic crystal fibers with flattened all-normal dispersion profile. Majority of research in SG is focused on obtaining the widest spectral bandwidth possible. The straightforward method for that is using a highly nonlinear PCF as the nonlinear medium, and a pump source operating at a wavelength close to the zero dispersion point on its anomalous dispersion side. Spectral broadening is then based on very efficient soliton-based dynamics and multi-octave spanning spectra have been reported in setups working in this regime [23–25]. The down side of soliton-based supercontinuum spectra are however their high susceptibility to laser shot noise, and low temporal stability [29]. An alternative approach to SG is exploiting broadening in the normal dispersion range of wavelengths, which precludes soliton formation and results in very stable and coherent broadening, albeit at a cost of bandwidth. Another important issue to address is the necessity to provide a nonlinear medium with a flattened normal dispersion profile, preferably with a local maxium at around intended pump wavelength. Using expertise in thermal matching of different glasses for structured fiber optic components, we recently demonstrated all-solid photonic crystal fibers with photonic lattice made of two types of thermally compatible glasses with different refractive indices and different dispersion profiles. Dispersion engineering in such structures is enabled with an additional degree of freedom against air-hole PCFs, since dispersion profile can be shaped not only by waveguide dispersion determined by the photonic microstructure, but also by resulting material dispersion of the two used glasses. All-solid PCFs with flattened, normal dispersion profiles optimized for SG pumping with wavelengths from the range of 1300–1600 nm have been recently reported by our group [30]. With a fiber from this series, shown in Fig. 34a, SG pumped with 120 fs pulses centered at 1360 nm (OPA) has been recorded covering spectral range of 900–1900 nm – Fig. 34c, [31]. The fiber was drawn from capillaries made of N-F2 glass and with central N-F2 rod for the core. The capillaries were filled with NC21 glass rods and the whole structure was inserted into an NC21 glass tube. Circular elements of the preform attained hexagonal shape during drawing. The drawn fiber had 137 μm in diameter, hexagonal photonic lattice was 35 μm in diagonal, capillary diagonal was $d = 2.1$ μm and lattice constant of $\Lambda = 2.3$ μm with resulting relative capillary size of $d/\Lambda = 0.91$. Solid N-F2 core had about 2.5 μm diameter. The dispersion characteristic of the fiber, calculated is shown in Fig. 34b along with SEM image of drawn fiber structure used for calculation. The dispersion profile was measured up to around 1700 nm. Both results are in good agreement, with small discrepancy for longer wavelengths, which can be assigned to diffusion of glasses in an

all-solid photonic structure. Another important advantage of all-solid PCFs for supercontinuum generation, demonstrated very recently [32] is that they can be spliced with relatively small losses, which creates a high potential for designing of efficient and robust all-fiber sources of coherent, broadband radiation.

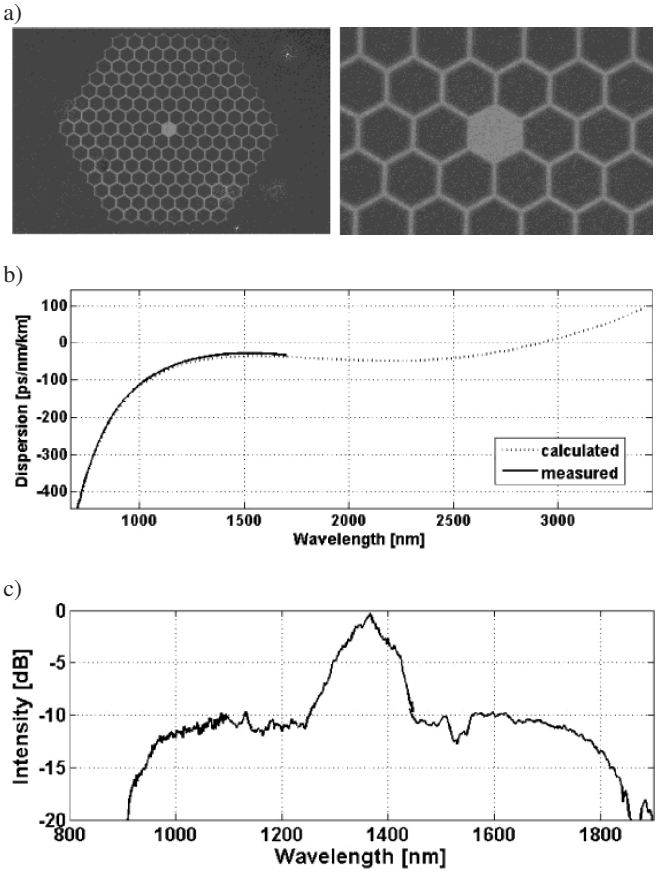

Fig. 34. a) SEM images of the all-solid photonic structure, b) calculated and measured dispersion profile of the PCF and c) measured supercontinuum spectrum pumped with 120 fs pulses and 50 nJ of incident energy (18% coupling efficiency into fiber) after Ref. 31

5. Conclusions

The stack-and-draw method, combined with recrystallization resistant glass synthesis technology, enables fabrication of a breadth of high quality microstructured fiber optic components, encompassing, but not limited to classic image guides, photonic crystal fibers and photonic bandgap fibers. The disposed state-of-the-art in structured fiber optics drawing technology enables designing and fabricating new types of microstructured fibers with complicated, asymmetric refractive index profiles, high nonlinearities or high birefringence, large mode areas or broadband, flattened dispersion profiles. Specialty structured fibers containing containing conducting, semiconductive, magnetostrictive elements, or metamaterials (with controlled permittivity and permeability, containing metal nanowires) are also investigated.

Acknowledgements. This work was supported by the project TEAM/2012-9/1 operated within the Foundation for Polish Science Team Programme co-financed by the European Regional Development Fund, Operational Program Innovative Economy 2007–2013 and by the Harmonia project UMO-2012/06/M/ST2/00479, funded by the National Science Centre in Poland.

REFERENCES

[1] L. Kociszewski, J. Buzniak, R. Stepien, and R. Romaniuk, "High quality image-guide by mosaic-assembling optical fiber technology", *Proc. SPIE* 906, 97–107 (1988).

[2] L. Kociszewski, R. Stepien, J. Buzniak, E. Poninska, and R. Romaniuk, "Basic properties and applications of advanced glass optical fibers", *ITME Works* 39, CD-ROM (1993).

[3] T. Tsumanuma, T. Tanaka, K. Seto, K. Sanada, and K. Inada, "New ultrathin needle scope used for diagnosis of small parts", *Proc. SPIE* 1067, 182–185 (1989).

[4] L. Kociszewski, D. Pysz, and R. Stępień, "Technological aspects of fiber optic integrated structures manufacturing", *Proc. SPIE* 3189, 22–26 (1997).

[5] D. Pysz, L. Kociszewski, and R. Stępień, "Technological aspects of fiber optic image guides for needle endoscopes manufacturing", *Proc. SPIE* 4158, 137–143 (2000).

[6] E. Silvestre, M.V. Andres, and P. Andres, "Biorthonormal-basis method for the vector description of optical-fiber modes", *J. Lightwave Techn.* 16 (5), 923–928 (1998).

[7] A. Ferrando, E. Silvestre, J.J. Miret, P. Andres, and M.V. Andres, "Full vector analysis of a realistic photonic crystal fiber modes", *Opt. Lett.* 24 (5) 276–278, (1999).

[8] A. Ferrando, E. Silvestre, J.J. Miret, P. Andres, and M.V. Andres, "Vector description of higher-order modes in photonic crystal fibers", *J. Opt. Soc. Am.* A 17 (7), 1333–1339 (2000).

[9] R. Buczynski, "Photonic crystal fibers", *Acta Physica Polonica* A 106 (2), 141–168 (2004).

[10] S. Ertman, T. R. Wolinski, D. Pysz, R. Buczynski, E. Nowinowski-Kruszelnicki, and R. Dabrowski, "Low-loss propagation and continuously tunable birefringence in high-index photonic crystal fibers filled with nematic liquid crystals", *Opt. Express* 17, 19298–19310 (2009).

[11] T. Li, *Optical Fiber Communications: Fiber Fabrication*, Academic Press, New York, 1997.

[12] P.M. Blanchard, J.G. Bernett, G.R.G. Erry, A.H. Greenaway, P. Harrison, B. Mangan, J.C. Knight, P.S. Russell, M.J. Gander, R. McBride, and J.D.C. Jones, "Two-dimensional bend sensing with a single multicore optical fiber", *Smart Matter Struct.* 9, 132–140 (2000).

[13] R. Buczynski, P. Szarniak, D. Pysz, I. Kujawa, R. Stepien, and T. Szoplik, "Double-core photonic crystal fiber with square lattice", *Proc. SPIE* 5450, 81–89 (2004).

[14] M.J. Steel and R.M. Osgood, Jr., "Elliptical-hole photonic crystal fibers", *Opt. Lett.* 26 (4), 229–231 (2001).

[15] R. Buczyński, P. Szarniak, D. Pysz, R. Stępień, and T. Szoplik, "Highly birefringent photonic crystal fibres with a square lattice", *Proc. SPIE* 5576, 92–97 (2004).

[16] P. Szarniak, R. Buczyński, D. Pysz, I. Kujawa, M. Franczyk, and R. Stępień, "Highly birefringent photonic crystal fibers with elliptical holes", *Photonic Crystals and Fibers: SPIE Int. Congress on Optics and Optoelectronics* 5950–58, CD-ROM (2005).

[17] R. Buczyński, D. Pysz, T. Ritari, P. Szarniak, H. Ludvigsen, and R. Stępień, "Optical properties of photonic band gap fibers made of silicate glass", *Proc. SPIE* 6182, 61821Z (2006).

[18] D. Pysz, I. Kujawa, R. Buczynski, A. Filipkowski, T. Martynkien, F. Berghmans, H. Thienpont, and R. Stepien, "Photonic band gap fiber with air dual core", *3rd Conf. Integrated Optics – Sensors, Sensing Structures and Methods* 1, CD-ROM (2009).

[19] I. Kujawa, R. Buczynski, D. Pysz, T. Martynkien, T. Nasilowski, H. Thienpont, and R. Stepien, "Silicate all-solid photonic crystal fibers with a glass high index contrast", *Proc. SPIE* 6588, 65880J (2007).

[20] D. Pysz, R. Buczynski, P. Szarniak, W.M. Saj, I. Kujawa, and R. Stepien, "Properties of photonic crystal fiber with double lattice of microholes and microrods", *Optical Fibers I: Technology: SPIE Int. Congress on Optics and Optoelectronics* 5951-05, CD-ROM (2005).

[21] R.R. Alfano and S.L. Shapiro, "Emission in the region 4000 to 7000 Å via four-photon coupling in glass", *Phys. Rev. Lett.* 24, 584–587 (1970).

[22] J. M. Dudley, G. Genty, and S. Coen, "Supercontinuum generation in photonic crystal fiber", *Rev. Mod. Phys.* 78 (4), 1135–1184 (2006).

[23] P. Domachuk, N.A. Wolchover, M. Cronin-Golomb, A. Wang, A.K. George, C.M.B. Cordeiro, J.C. Knight, and F.G. Omenetto, "Over 4000 nm bandwidth of mid-IR supercontinuum generation in sub-centimeter segments of highly nonlinear tellurite PCFs", *Opt. Express* 16 (10), 7161–7168 (2008).

[24] O. Mouawad, J. Picot-Clémente, F. Amrani, C. Strutynski, J. Fatome, B. Kibler, F. Désévédavy, G. Gadret, J.-C. Jules, D. Deng, Y. Ohishi, and F. Smektala, "Multioctave midinfrared supercontinuum generation in suspended-core chalcogenide fibers", *Opt. Lett* 39 (9), 2684–2687 (2014).

[25] A.M. Heidt, J.H.V. Price, C. Baskiotis, J.S. Feehan, Z. Li, S.U. Alam, and D.J. Richardson, "Mid-infrared ZBLAN fiber supercontinuum source using picosecond diode-pumping at 2 μm", *Opt. Express* 21 (20), 24281–24287 (2013).

[26] M. Klimczak, G. Stepniewski, H. Bookey, A. Szolno, R. Stepien, D. Pysz, A. Kar, A. Waddie, M.R. Taghizadeh, and R. Buczynski, "Broadband infrared supercontinuum generation in hexagonal-lattice tellurite photonic crystal fiber with dispersion optimized for pumping near 1560 nm", *Opt. Lett.* 38 (22), 4679–4682 (2013).

[27] M. Klimczak, B. Siwicki, P. Skibinski, D. Pysz, R. Stepien, A. Szolno, J. Pniewski, C. Radzewicz, and R. Buczynski, "Mid-infrared supercontinuum generation in soft-glass suspended core photonic crystal fiber", *Optical and Quantum Electronics* 46 (4), 563–571 (2014).

[28] G. Sobon, M. Klimczak, J. Sotor, K. Krzempek, D. Pysz, R. Stepien, T. Martynkien, K. M. Abramski, and R. Buczynski, "Infrared supercontinuum generation in soft-glass photonic crystal fibers pumped at 1560 nm", *Optical Materials Express* 4 (1), 7–15 (2014).

[29] A. M. Heidt, A. Hartung, G.W. Bosman, P. Krok, E.G. Rohwer, H. Schwoerer, and H. Bartelt, "Coherent octave spanning near-infrared and visible supercontinuum generation in all-normal dispersion photonic crystal fibers", *Opt. Express* 19 (4), 3775–3787 (2011).

[30] T. Martynkien, D. Pysz, R. Stępień, and R. Buczyński, "All-solid microstructured fiber with flat normal chromatic dispersion", *Opt. Lett.* 39 (8), 2342–2345 (2014).

[31] G. Stepniewski, M. Klimczak, H. Bookey, B. Siwicki, D. Pysz, R. Stepien, A.K. Kar, A.J. Waddie, M.R. Taghizadeh, and R. Buczynski, "Broadband supercontinuum generation in normal dispersion all-solid photonic crystal fiber pumped near 1300 nm", *Laser Physics Letters* 11 (5), 055103 (2014).

[32] M. Murawski, G. Stępniewski, T. Tenderenda, M. Napierała, Z. Hołdyński, L. Szostkiewicz, M. Slowikowski, M. Szymanski, L. Ostrowski, L.R. Jaroszewicz, R. Buczyński, and T. Nasiłowski, "Low loss coupling and splicing of standard single mode fibers with all-solid soft-glass microstructured fibers for supercontinuum generation", *Proc. SPIE* 8982, 898228-1 (2014).